International Journal of Heat and Mass Transfer 194 (2022) 123021

Contents lists available at ScienceDirect

International Journal of Heat and Mass Transfer

journal homepage: www.elsevier.com/locate/hmt

# On the two-temperature description of heterogeneous materials

R. Kovács [a,b,c,*], A. Fehér [a], S. Sobolev [d]

[a] Department of Energy Engineering, Faculty of Mechanical Engineering, Budapest University of Technology and Economics, Mũegyetem rkp. 3., H-1111 Budapest, Hungary
[b] Department of Theoretical Physics, Wigner Research Centre for Physics, Institute for Particle and Nuclear Physics, Budapest, Hungary
[c] Montavid Thermodynamic Research Group, Budapest, Hungary
[d] Institute of Problems of Chemical Physics, Academy of Sciences of Russia, Moscow Region, Russia

ARTICLE INFO

*Article history:*
Received 5 February 2022
Revised 1 April 2022
Accepted 10 May 2022

*Keywords:*
Two-temperature model
Guyer-Krumhansl equation
Nonequilibrium thermodynamics
Heterogeneous materials

ABSTRACT

The thermal behaviour is critical in numerous applications, affecting any device's lifetime and safe operations. Adding that the technological development resulted in the appearance of complex material structures, making the research on advanced thermal models even more important. Materials like 3D printed structures, foams, or with a biological origin often show non-Fourier thermal response. Modelling such a problem requires a thorough analysis and a deep understanding of non-Fourier models. The present paper focuses on two advanced models, called two-temperature and Guyer-Krumhansl equations. We compare their physical background and characteristic behaviour. Additionally, we perform the first experimental test of the two-temperature model. It is found that the solutions of the two-temperature model deviate from the ones predicted by the Guyer-Krumhansl equation. However, both approaches can model the experimental data under certain conditions and offer different insights about the observed heat conduction phenomenon.



## 1. Introduction

In the last decades, there has been a tendency to design the material structure for a particular application, and such materials are foams, composites, and metamaterials. Additionally, various heterogeneities are also present due to the manufacturing procedure, e.g., for 3D printed objects for which the object is formed from particles, thus having a microporous structure. The present paper focuses on the thermal characterisation of heterogeneous materials, considering only isotropic and constant material parameters.

The recent experimental findings [1,2] suggest that heterogeneous materials can show thermal behaviour different from Fourier's law at room temperature in a macroscale object. That deviation is not similar to second sound or ballistic propagation, i.e., no wavefronts are observed in the measurements. Instead, it occurs due to the presence of parallel heat conduction channels. The difference in the heat conduction channels originates in the heterogeneity. For instance, the bulk metal material in a metal foam sample has good conductivity properties, while the gaseous material in the inclusions is more similar to an insulator. Furthermore, thermal radiation and heat convection could also contribute to the thermal behaviour, meaning further difficulties in the modelling. However, the situation is different for a rock sample, where the presence of various constituents and porosity together realise the non-Fourier thermal response.

That phenomenon is called over-diffusive propagation and has the following characteristics, presented on a usual experimental observation. Figure 1 presents a typical rear side temperature history for a heat pulse experiment, using a metal foam sample [3]. First, the temperature rise is faster compared to Fourier's prediction. Around the top, that faster increase of temperature diminishes; instead, it becomes slower. This observation suggests the existence of two characteristic time scales for which the Fourier equation presents their average [2]. However, a more advanced model can provide a finer resolution about this phenomenon, including both time scales and therefore presenting a better explanation with a predictive nature.

* Corresponding author at: Department of Energy Engineering, Faculty of Mechanical Engineering, Budapest University of Technology and Economics, Mũegyetem rkp. 3., H-1111 Budapest, Hungary.
*E-mail address:* kovacs.robert@wigner.mta.hu (R. Kovács).

https://doi.org/10.1016/j.ijheatmasstransfer.2022.123021

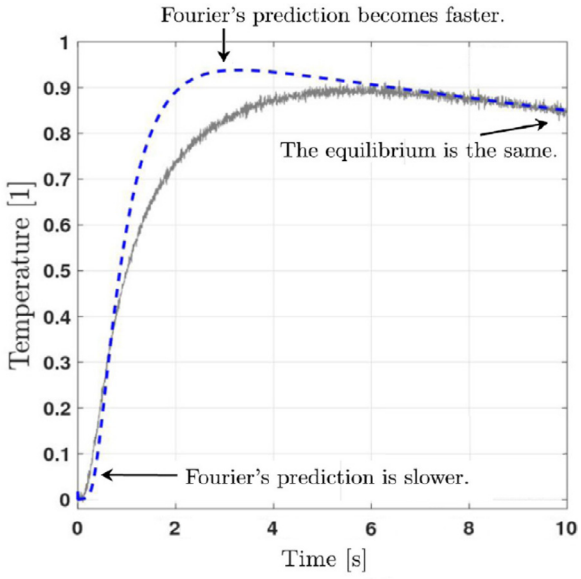


**Fig. 1.** The normalised rear side temperature history for a metal foam sample together with its best Fourier fit [3].

It is clear that a model is not practically advantageous with including specific material properties (e.g., the distribution and size of inclusions) as it strictly restricts the range of validity. This approach is, however, typical for biological problems in which more and more geometrical details are included. For instance, for a skin thermal model, it is natural to present the different layers, the vascular network, fat distribution and so on [4–6]. In the end, the model becomes complex with many uncertain parameters, such as the thermal contact resistances on the interfaces. Additionally, these attributes differ from person to person, and hence there is a natural variance in the parameters. While a detailed model increases the computational costs, it does not increase the accuracy of the prediction as the key factors bear a natural, uncontrollable variance [7]. Consequently, instead of focusing on the specific material structure, we utilise models in which the two time scales are present and characterise the thermal behaviour effectively.

That effective description neglects the inner properties, and therefore the resulting parameters represent 'average' values. These values, however, could be size-dependent, and that stands as an additional challenge for experiments [2]. Whether a measurement method or a particular application presents particular size limits on the objects, size dependence can occur in many situations. We do not aim to investigate this property here, but we feel it essential to keep in mind and call attention to these difficulties.

In the present paper, we focus on two thermal modelling approaches developed for heterogeneous materials and test them on experiments. The first one is the application of the Guyer-Krumhansl (GK) equation, used earlier in numerous occasions with success [2,8]. The second one, called the two-temperature (2T) approach [9–11], however, has not been tested on heat pulse experiments so far but has a promising background and could influence, e.g., the thermoelectric conversion processes [12]. The 2T model has been successfully used for heat transport in metals under ultrashort heat pulses [13–16], and also investigated by Gonzalez-Vázquez et al. [17]. Therefore, we aim to thoroughly investigate the properties of the 2T model and compare its outcome to the results of the GK equation. We note that many other heat equations can be found in the literature [18–22], but they are not tested or not applicable for macroscale solids at room temperature. Many of them particularly attributed to low-temperature phenomena such as second sound and ballistic heat conduction [23–27].

## 2. Thermal models with two time scales

### 2.1. 2T model

Let us suppose that the heterogeneous material can be divided into two subsystems. These subsystems obey the Fourier law and can interact with each other, and that model can express the existence of parallel heat conduction channels. Therefore, the entire system is characterised by two diffusivities, presenting two distinct characteristic time scales. Such a situation can occur, e.g., in plasma, for which the electrons and ions represent the subsystems or in a sandwich structure including two distinct components. Thus the model reads in one spatial dimension as

$$\rho_i c_i \partial_t T_i + \partial_x q_i = (-1)^j g(T_j - T_i), \tag{1}$$

$$q_i = -\lambda_i \partial_x T_i, \quad (i = \{1,2\}, \ \ j = \{1,2 \mid j \neq i\}), \tag{2}$$

where $\rho$, $c$, $\lambda$, $T$, $q$ are the mass density, specific heat, thermal conductivity, temperature and heat flux for the corresponding subsystem, respectively. Furthermore, $\partial$ denotes the partial derivative respect to time ($t$) or space ($x$). The source term expresses the heat exchange between the subsystems, hence $g$ is a sort of 'inner heat transfer coefficient', being uniform in the domain of interest. The indices $i$ and $j$ denote the corresponding subsystem, and the sign alters in the source term by taking $(-1)^j$. Equation (1) represent the balance of internal energy ($e$) in which $e = cT$ is exploited, and no further source terms are included. Equation (2) is a constitutive equation, called Fourier's law. In non-Fourier models, Eq. (2) is exchanged with a partial differential equation, which has numerous consequences [28]. From now on, we consider all parameters constant. For simplicity, we introduce the notation $C_i = \rho_i c_i$. That model describes a purely heat conduction phenomenon, without any coupling to mechanics. Moreover, the subsystems are only coupled through the balance equation, the constitutive equations are not connected.

Following [8–10,29], there are two different temperature representations of such system. First, one can express $T_i$, which is

$$\tau \partial_{tt} T_i + \partial_t T_i = \alpha_i \partial_{xx} T_i + l^2 \partial_{txx} T_i - \alpha_g l_g^2 \partial_{xxxx} T_i, \tag{3}$$

in which

$$\tau = \frac{C_1 C_2}{g(C_1 + C_2)}, \quad \alpha_i = \frac{\lambda_i}{C_i}, \quad l^2 = \tau(\alpha_1 + \alpha_2), \quad \alpha_g = \frac{l_g^2}{\tau},$$
$$l_g^2 = \tau\sqrt{\alpha_1 \alpha_2}, \quad (g \neq 0), \tag{4}$$

wherein $\alpha_i$ denotes the thermal diffusivity of the corresponding subsystem, and $\tau$ is the characteristic time of energy exchange between the subsystems. Second, one can also choose to use the average temperature $\bar{T} = (C_1 T_1 + C_2 T_2)(C_1 + C_2)^{-1}$, that is,

$$\tau \partial_{tt} \bar{T} + \partial_t \bar{T} = \alpha_i \partial_{xx} \bar{T} + l^2 \partial_{txx} \bar{T} - \alpha_g l_g^2 \partial_{xxxx} \bar{T}, \tag{5}$$

where the coefficients defined through (4).

### 2.2. GK model

The Guyer-Krumhansl equation was first derived as a linearization of the Boltzmann equation [30]. Phonon hydrodynamics is not applicable for solids in room temperature macroscale situations, therefore the approach of Rational Extended Thermodynamics [26,31] is excluded. Here, we consider the continuum thermodynamic background [32–34], for which the coefficients are restricted only by the second law of thermodynamics. On the contrary to the kinetic theory [35], there is no prior assumption on the heat conduction mechanism, therefore, it becomes possible to find the parameters from an experiment analogously to the Fourier equation. Consequently, this GK model we apply has the same

structure but is different in interpreting the coefficients from the original one. That attribute extends the range of validity, and the GK equation is found to be helpful to characterise heterogeneous materials [36].

The GK constitutive equation reads in one spatial dimension,

$$\tau\,\partial_t q + q = -\lambda\,\partial_x T + l^2\,\partial_{xx} q, \tag{6}$$

where the coefficients cannot be interpreted as Eq. (4) suggests, they found directly from a measurement. Considering again a linear model, the temperature representation of the GK equation is

$$\tau\,\partial_{tt} T + \partial_t T = \alpha\,\partial_{xx} T + l^2\,\partial_{txx} T, \tag{7}$$

from which the last term of Eq. (5) is missing. In other words, the similarity between Eqs. (3) and (6) is only formal, they possess different physical meaning, therefore the coefficients Eq. (4) is not valid for (7), instead, the coefficients of (7) is found by fitting to a transient measurement. Using this $T$-representation, it becomes visible that the GK equation also consists of two time scales with two diffusivities: $\alpha$ and $l^2/\tau$. Based on the relationship between these coefficients, one can distinguish three characteristic domains: under-diffusive ($\alpha > l^2/\tau$), over-diffusive ($\alpha < l^2/\tau$), and Fourier resonance ($\alpha = l^2/\tau$) [37,38]. Under-diffusive behaviour results in a damped wave propagation, and is characteristic for the low-temperature problems. In our situation, the over-diffusive propagation is of great importance, together with the Fourier resonance. While there are common points and similarities between these models, their constitutive background significantly differs, which leads to severe consequences on the mathematical and physical interpretation of the results.

### 2.3. Initial and boundary conditions

In order to solve these heat conduction models, one needs to define initial and boundary conditions. Their definitions depend on the model, and therefore, they are different for the 2T and GK approaches.

For a 2T model, one must define the initial temperature distribution for both subsystems. In the case of a space-dependent initial condition, the Fourier law can be used to determine the heat flux at the initial time instant. It requires detailed knowledge about each subsystem, which could be a restrictive property. For the GK equation, however, one also needs the initial time derivative of the temperature field. This can be determined using the GK constitutive equation. These differences are crucial for nonequilibrium initial states.

In regard to the boundary conditions, the differences are more significant as they do not require special situations. The boundary conditions are defined through the constitutive equations to preserve physical consistency. Therefore, for a 2T model, one may define the classical, well-known boundary conditions for the subsystems, depending on the situation. Moreover, the boundary conditions can differ for the subsystems, although they are not straightforward. For instance, considering a heterogeneous sample in a heat pulse experiment, it is not clear whether the heat pulse excites both subsystems or how the overall heat input splits between them. Analogously, for Neumann-type boundary conditions, determining the heat transfer coefficients is also not a straightforward question. These are crucial aspects in a 2T model. On the contrary, the GK equation is free from this difficulty; instead, it introduces other aspects. Since the GK constitutive Eq. (6) introduces additional time and space derivatives of heat flux, the temperature gradient is no longer capable of prescribing heat flux-type boundary conditions. In other words, its $T$-representation (7) is only helpful for Dirichlet boundaries. For Neumann-type boundary conditions, a $q$ or a mixed (without eliminating any variables) representation is recommended [29]. This is a key aspect of solving the GK equation.

### 2.4. Nonlinearities

Here, we restrict ourselves to the temperature-dependent parameters, as it is an essential question for practical applications. In that sense, the 2T model follows the classical methodology. Additionally, $\rho_i$, $c_i$, and $\lambda_i$ can depend only on $T_i$. The situation is more difficult for the GK model due to the complex constitutive equation. As a consequence of the second law of thermodynamics, the parameters $\tau$, $\lambda$, and $l^2$ are not independent of each other, i.e.,

$$\tau = \frac{\rho m}{k_2}, \quad \lambda = \frac{1}{k_2 T^2}, \quad l^2 = \frac{k_1}{k_2} \tag{8}$$

form the coefficients of the GK equation according to the Onsagerian relations ($k_1, k_2, m \geq 0$) [34]. In general, the coefficients $k_1$, $k_2$ and $m$ are positive definite functions of state variables. However, in numerous situations, the linear approximation is sufficient, thus they considered to be (positive) constants. Nevertheless, when the thermal conductivity $\lambda$ depends on the temperature (by $k_2 = k_2(T)$), it immediately introduces temperature dependence into all the other parameters, since $k_2$ contributes for $\tau$ and $l^2$ as well [39]. It has further consequences: such temperature dependence modifies the system of evolution equations, and mechanics is also involved through thermal expansion [39,40].

This is a significant difference between these approaches, and it is entirely missing from the models based on the dual-phase-lag (DPL) approach [41]. While the DPL model

$$q(x, t + \tau_q) = -\lambda\,\partial_x T(x, t + \tau_T) \tag{9}$$

has numerous variants based on the order of the Taylor series expansion [42–44] and being popular due to its simple background, but it lacks the proper physical background and leading to ill-posed problems [45–50]. However, in a particular situation, the DPL model can reduce to a hyperbolic heat conduction equation when $\tau_T \to 0$, or analogously, when $\tau_T < \tau_q$. This hyperbolic model is often identified as the Cattaneo-Vernotte (CV) [51,52] equation, but the DPL model can lead to other hyperbolic equations as well with higher-order Taylor expansions. The thermodynamically compatible version of the DPL equation is called Jeffreys equation [34,53]

$$\tau\,\partial_t q + q = -\lambda\Big(\partial_x T + \tau\,\partial_{xt} T\Big), \tag{10}$$

where only one relaxation time appears on contrary to the DPL Eq. (9), and the coefficient of $\partial_{xt} T$ cannot be arbitrary. Furthermore, its T-representation shows similarities to both 2T and GK models:

$$\tau\,\partial_{tt} T + \partial_t T = \alpha\,\partial_{xx} T + \alpha\tau\,\partial_{txx} T, \tag{11}$$

in which the coefficients differ from the other approaches, therefore the time scales can also be interpreted differently. The Jeffreys model is closest to the GK equation, however, as the constitutive Eq. (10) consists of $\partial_{tx} T$ instead of $\partial_{xx} q$, it significantly affects every attributes, including the initial and boundary conditions, too. Clearly, a solid thermodynamic background can be a reliable guide to consistently include the necessary nonlinearities. Furthermore, Mariano et al. also suggest further modifications on the CV equation using microstructural aspects [54,55].

## 3. Characteristic solutions of the 2T model

Here, we aim to present the characteristics of the 2T model in comparison to the GK equation. We apply initial and boundary conditions corresponding to the heat pulse measurement technique for which the experimental test of the 2T model can be achieved. Therefore, the initial conditions describe a steady-state,

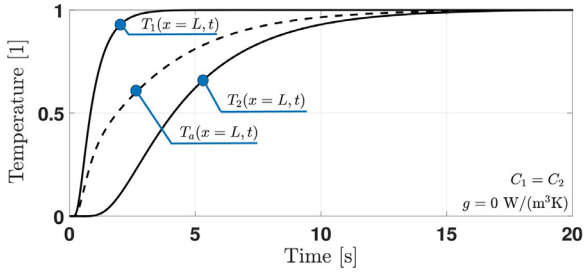


**Fig. 2.** The normalised rear side temperature history according to the 2T model, $T_a$ denotes the average temperature. The parameters: $\rho_1 = \rho_2 = 2700$ kg/m$^3$; $c_1 = c_2 = 900$ J/(kgK); $\lambda_1 = 10$ W/(m·K), $\lambda_2 = 2$ W/(m·K), and $g = 0$ W/(m$^3$K).

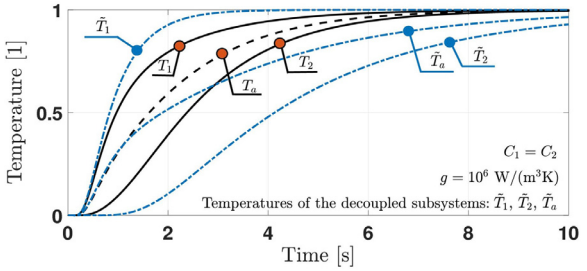


**Fig. 3.** The normalised rear side temperature history according to the 2T model, $T_a$ denotes the average temperature. The parameters: $\rho_1 = \rho_2 = 2700$ kg/m$^3$; $c_1 = c_2 = 900$ J/(kgK); $\lambda_1 = 10$ W/(m·K), $\lambda_2 = 2$ W/(m·K), and $g = 10^6$ W/(m$^3$K).

i.e.,

$$\text{2T model:} \quad q_i(x, t=0) = 0 \ \frac{W}{m^2}, \quad T_i(x, t=0) = T_0, \quad (i = 1, 2) \tag{12}$$

$$\text{GK model:} \quad q(x, t=0) = 0 \ \frac{W}{m^2}, \quad T(x, t=0) = T_0 \tag{13}$$

with $T_0$ being a uniform initial temperature distribution, and is equal to the ambient temperature, too. The boundary conditions are

$$\text{2T model:} \quad q_i(x=0, t \le t_p) = q_0\left(1 - \cos\left(\frac{2\pi t}{t_p}\right)\right) \frac{W}{m^2},$$
$$q_i(x=L, t) = h(T(x=L,t) - T_0)\frac{W}{m^2}, \quad (i = 1, 2) \tag{14}$$

$$\text{GK model:} \quad q(x=0, t \le t_p) = q_0\left(1 - \cos\left(\frac{2\pi t}{t_p}\right)\right) \frac{W}{m^2},$$
$$q(x=L, t) = h(T(x=L,t) - T_0)\frac{W}{m^2} \tag{15}$$

in which it is assumed that $q_1$ and $q_2$ have the same boundary conditions in the 2T model, i.e., the subsystems equally receive the heat pulse during its time $t_p$. After the heat pulse, the boundaries are adiabatic for both models at the front, i.e., $q(x, t \ge t_p) = 0$ W/m$^2$. At the rear end, we can use convection boundary condition with the heat transfer coefficient $h$, assumed to be the same for both subsystems and for both models. Although, different constitutive equations might lead to different heat transfer coefficients, but $h$ also significantly depends on the environmental conditions and boundary layer properties. Therefore, assuming the same $h$ for different models implies that we assume the same environmental conditions, which is practically feasible in heat pulse experiments due to the closed measurement chamber. Furthermore, as $h$ depends on the surrounding fluid boundary layer, we can safely assume that Fourier's law remains valid, thus the Nusselt equation is not modified, and the same heat transfer coefficient could be a practically viable situation.

Both models are solved numerically with the procedure described in [56], using the finite difference method with staggered spatial discretization. This procedure is validated by analytical solutions in the case of the GK equation with the given set of initial and boundary conditions [29].

Figure 2 presents the most straightforward situation with the 2T model, where both heat capacities ($C_1$ and $C_2$) are equal, and the coupling heat transfer coefficient ($g$) is considered to be zero together with the heat transfer coefficient. It means that the subsystems are decoupled in the entire domain, but it is still possible to take their average at the end. It has experimental importance since it can be easily realised using a thin silver layer at the end [1]. However, in that case, the coefficients ($\tau$, $\alpha$ and $l^2$) cannot

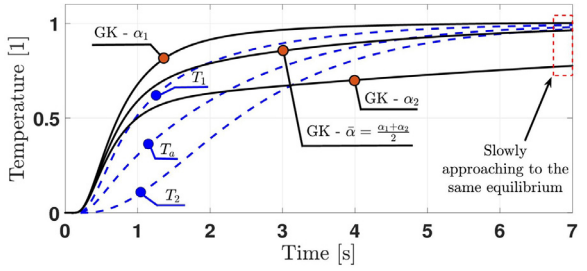


**Fig. 4.** The normalised rear side temperature histories of the GK and 2T models. The same set of parameters ($\tau = 1.215$ s, $l^2 = 6 \cdot 10^{-6}$ m$^2$) is utilised for the GK Eq. (6) and the 2T model (3).

be directly connected to the GK model based on (4). The qualitative behaviour changes significantly when the coupling is active (i.e., $g \neq 0$). Figure 3 represents the case when $g = 10^6$ W/(m$^3$K) is applied, which is chosen to achieve a realistic relaxation time $\tau = 1.215$ s, found in recent experiments, being characteristic for the rock samples [2].

Figure 4 compares the outcomes of both models for that set of parameters ($l^2 = 6 \cdot 10^{-6}$ m$^2$). The GK equation is solved for three different thermal diffusivities. In two cases, the thermal diffusivity of the corresponding subsystem ($\alpha_1$ and $\alpha_2$) are utilised. Their average ($\bar{\alpha}$) is substituted in the third one. Visibly, the GK equation produces significantly different outcomes in each case. The reasons can be found in their physical background. These equations model a different physical situation. They are analogous, but their outcome is not the same. While the 2T model remains valid for $g = 0$, and the average temperature is still meaningful, it cannot be compared to the GK equation as $\tau \to \infty$. Furthermore, the interpretation of their boundary conditions is also different. Overall, despite (3) and (5), these models remain only similar but cannot be the same, especially due to the additional term ($\partial_x^4 T$) in the 2T model.

## 4. Experimental aspects

The heat pulse measurement is used as a standard method to determine the thermal diffusivity of a material by recording the rear side temperature history [57], Fig. 5/A) shows the arrangement of the measurement schematically. In order to test the experimental capabilities of the 2T model, we aim to reproduce these rear side temperature histories recorded recently for a metal foam [3] and a rock sample [2].

However, the 2T model consists of numerous parameters to fit, and their number depends on how the model is utilised. First, as we have seen in the previous section, it is not possible to use the GK parameters and calculate the coefficients in the 2T model using (4) since the models do not cover the same physical system. Therefore, Eqs. (3) and (5) are not advantageous. Second, if the 2T model

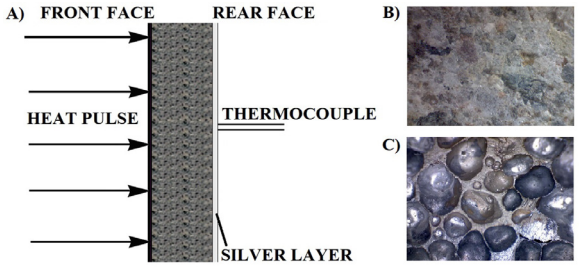


**Fig. 5.** A) The schematics of the experimental setup [1]. B) The magnified image of the Szaszvar formation rock sample. C) The magnified image of the metal foam sample.

is exploited in its original form, see Eqs. (1)-(2)), then 6 material parameters, 1 coupling coefficient and 1 heat transfer coefficient are to be found, 8 altogether. The 6 material parameters can be reduced to 4 if only the heat capacities $C_i$ are found instead of $\rho_i$ and $c_i$. There is a third way, where the two heat equations in the 2T model are solved in the form of

$$\partial_t T_i = \alpha_i \partial_{xx} T_i + \frac{(-1)^j g}{\rho_i c_i}(T_j - T_i), \quad (i = \{1,2\}, \ j = \{1,2 \mid j \neq i\}). \tag{16}$$

That way, the fitting of the parameters $\alpha_i$ and $\chi_i = g/(\rho_i c_i)$ are not enough to recover the complete set of parameters if the temperature averaging is used since it needs $C_i$ as well. The efficient fitting of 8 parameters would require a complex procedure, which is not yet developed for the 2T model. Moreover, as the number of parameters is twice as much as for the GK model, it needs further investigation to avoid overfitting. The possibility to take the average of the temperature of the subsystems $T_i$, making the situation even more difficult. Consequently, the data we publish here is only an approximation, a basic test of whether the capability of the 2T model is present or not, before developing an advanced technique. Additionally, it would not be conclusive to statistically compare the fittings to each other since there is no any elaborated fitting approach for the 2T model, which would require a thorough parameter investigation. Regarding the GK equation, an efficient evaluation method is developed based on an analytical solution [8], where the GK parameters are found analogously to the case of the Fourier heat equation.

*Test I. - Szaszvar formation*

The magnified image of the rock sample is presented in Fig. 5/B). It has a cylindrical shape with a diameter of 25 mm, and its thickness is 3.8 mm. As highlighted in Fig. 5/A), there is a silver layer at the rear side. This is used to realise a proper contact for the thermocouple, and consequently, Fig. 6 shows the temperature of that silver layer. From the point of view of the 2T model, that silver layer performs the averaging, therefore it is reasonable to fit the average temperature $\bar{T}$. Interestingly, the fit depicted in Fig. 6 is found with $g = 0$ W/(m$^3$K), therefore, the $\tau$ and $l^2$ parameters cannot be compared to the ones from the GK equation. Despite that these models are not comparable on the level of equations and parameters, both of them can interpret and model the same experimental data. For simplicity, we assumed that both components have the same heat capacity $C_i$, thus both subsystems contribute equally to the averaging. This is, naturally, a factor that can distort the results. However, no data is available on the constituents of the rock sample. This uncertainty is a weak point of the fitting and the 2T model. The two thermal diffusivities are $\alpha_1 = 1.178 \cdot 10^{-6}$ m$^2$/s, and $\alpha_1 = 0.7111 \cdot 10^{-6}$ m$^2$/s. Their average is $\bar{\alpha} = 0.944 \cdot 10^{-6}$ m$^2$/s, which is close to the one found with the GK equation: $\alpha_{GK} = 0.922 \cdot 10^{-6}$ m$^2$/s [8]. Additionally, the GK parameters are $\tau = 0.648$ s, and $l^2 = 0.715 \cdot 10^{-6}$ m$^2$. Consequently, the 2T model would be more advantageous for subsystems with known inner structure and material properties.

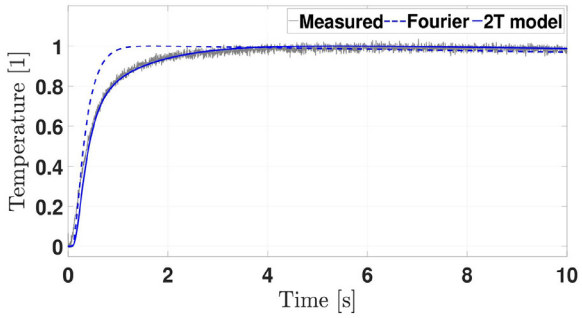


**Fig. 6.** The normalised rear side temperature history for the Szaszvar formation. The parameters: $\rho_1 = \rho_2 = 2500$ kg/m$^3$; $c_1 = c_2 = 900$ J/(kgK); $\lambda_1 = 2.65$ W/(m·K), $\lambda_2 = 1.6$ W/(m·K), $h = 13$ W/(m$^2$K), $g = 0$ W/(m$^3$K).

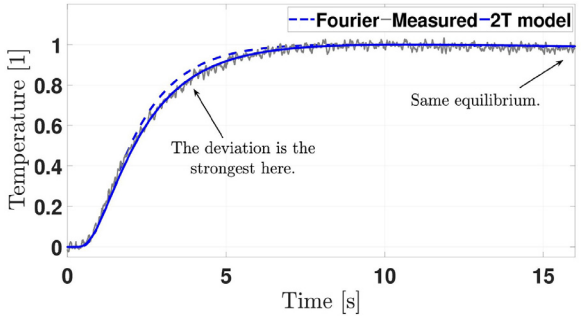


**Fig. 7.** The normalised rear side temperature history for the metal foam sample. The parameters: $\rho_1 = \rho_2 = 2700$ kg/m$^3$; $c_1 = c_2 = 900$ J/(kgK); $\lambda_1 = 24$ W/(m·K), $\lambda_2 = 2$ W/(m·K), $h = 9.8$ W/(m$^2$K), $g = 1.6 \cdot 10^6$ W/(m$^3$K).

*Test II. - Metal foam*

The magnified image of the metal foam sample is presented in Fig. 5/C), which has a thickness of 5.2 mm. The recorded temperature history, however, shows the evolution of $T_1$. This is reasonable since only the temperature of the bulk material can be measured, there is no averaging. While the Fourier thermal diffusivity is $\alpha_F = 1.2 \cdot 10^{-5}$ m$^2$/s, it is found that the subsystems have significantly lower values, i.e., $\alpha_1 = 9.87 \cdot 10^{-6}$ m$^2$/s, and $\alpha_2 = 0.823 \cdot 10^{-6}$ m$^2$/s. In the case of over-diffusive heat conduction, the GK thermal diffusivity is always found to be smaller than Fourier's [2]. The present set of parameters lead to $\tau_{2T} = 0.76$ s, and $l^2_{2T} = 8.125 \cdot 10^{-6}$ m$^2$, according to Eq. (4). The prediction of the GK equation falls into the same order of magnitude, that is, $\tau_{GK} = 0.4$ s, and $l^2_{GK} = 2.89 \cdot 10^{-6}$ m$^2$ (Fig. 7).

## 5. Discussion

Two advanced models are presented, the 2T and the GK equations. Based on the first test of the 2T model, it is clear that both approaches can model the same phenomenon. However, there are elementary differences, which have several severe consequences on the outcome.

First, we have seen that the initial and boundary conditions can differ from each other. For a 2T model, we needed the assumption that both subsystems receive the same amount of heat. We also exploited this attribute for the metal foam sample since there are inclusions right below the surface as well. This could be significantly different in reality. Additionally, we also assumed that the

heat capacities are equal, which could be a viable option in some instances. Second, the 2T model needs information about the material structure, especially about the constituents. Otherwise, the 2T model doubles the number of parameters and makes the fitting procedure notably more difficult. Furthermore, the 2T model requires a reliable and effective evaluation procedure, probably based on an analytical solution that could ease the fitting, at least the first guess for the parameters. Third, the 2T model needs input about the measurement technique itself, which is demonstrated through the previous tests. It does matter which temperature is measured in an experiment, and it explicitly appears in the 2T model. It is an essential advantageous property, which is missing from any other models. However, with the present 8 parameters in the 2T model, the fitting might not be unique, at least when only the rear side temperature history is investigated. Therefore, in regard the experimental techniques, we propose to record the temperature also on the front and on the lateral sides of the sample. These would serve as further constraints in the fitting procedure that would help to find the parameters reliably.

It is important that a model should be predictive for practical applications. For instance, when one designs a composite structure, it is easier to estimate the characteristic time scales using the 2T model, as it couples two Fourier heat equations. However, the design of the coupling parameter would be challenging as it depends on several factors, similarly to a heat transfer coefficient. Both thermal models require further experimental and theoretical investigation as it is still an open question how the parameters depend on the material structure. Additionally, the 2T model is not restricted to the case of two coupled Fourier equations. It could be possible to couple the Fourier equation to a more general model such as the GK equation, providing an approach for more complex heat conduction phenomena. For instance, the approach of Chen [25] can be investigated in the future in regard the presented physical and mathematical aspects.

## Declaration of Competing Interest

The authors declare that they have no known competing financial interests or personal relationships that could have appeared to influence the work reported in this paper.

## Acknowledgement

We thank László Kovács (ROCKSTUDY Ltd. (Kõmërõ Kft.), Hungary) and Tamás Bárczy (Admatis Kft., Hungary) for producing the rock and metal foam samples. The research reported in this paper and carried out at BME has been supported by the grants National Research, Development and Innovation Office-NKFIH FK 134277, by the NRDI Fund (TKP2020 NC, Grant No. BME-NC) based on the charter of bolster issued by the NRDI Office under the auspices of the Ministry for Innovation and Technology and the New National Excellence Program of the Ministry for Innovation and Technology project ÚNKP-21-5-BME-368. This paper was supported by the János Bolyai Research Scholarship of the Hungarian Academy of Sciences. S.L. Sobolev acknowledges that he works in accordance with the state task of Russian Federation, state registration No. AAAA-A19-119071190017-7.

## References

[1] S. Both, B. Czél, T. Fülöp, G. Gróf, A. Gyenis, R. Kovács, P. Ván, J. Verhás, Deviation from the Fourier law in room-temperature heat pulse experiments, J. Non-Equilib. Thermodyn. 41 (1) (2016) 41–48.
[2] A. Fehér, N. Lukács, L. Somlai, T. Fodor, M. Szücs, T. Fülöp, P. Ván, R. Kovács, Size effects and beyond-fourier heat conduction in room-temperature experiments, J. Non-Equilib. Thermodyn. 46 (2021) 403–411.
[3] P. Ván, A. Berezovski, T. Fülöp, G. Gróf, R. Kovács, A. Lovas, J. Verhás, Guyer-Krumhansl-type heat conduction at room temperature, EPL 118 (5) (2017) 50005. ArXiv:1704.00341v1
[4] H.G. Klinger, Heat transfer in perfused biological tissue–I: general theory, Bull. Math. Biol. 36 (1974) 403–415.
[5] P. Hooshmand, A. Moradi, B. Khezry, Bioheat transfer analysis of biological tissues induced by laser irradiation, Int. J. Therm. Sci. 90 (2015) 214–223.
[6] E.P. Scott, M. Tilahun, B. Vick, The question of thermal waves in heterogeneous and biological materials, J. Biomech. Eng. 131 (7) (2009) 074518.
[7] A. Sudár, G. Futaki, R. Kovács, Continuum modeling perspectives of non–fourier heat conduction in biological systems, J. Non-Equilib. Thermodyn. 46 (4) (2021) 371–381.
[8] A. Fehér, R. Kovács, On the evaluation of non-Fourier effects in heat pulse experiments, Int. J. Eng. Sci. 169 (2021) 103577 ArXiv:2101.01123.
[9] S.L. Sobolev, Heat conduction equation for systems with an inhomogeneous internal structure, J. Eng. Phys. Thermophys. 66 (4) (1994) 436–440.
[10] S.L. Sobolev, Local non-equilibrium transport models, Phys. Usp. 40 (10) (1997) 1043–1053.
[11] S.L. Sobolev, Nonlocal two-temperature model: application to heat transport in metals irradiated by ultrashort laser pulses, Int. J. Heat Mass Transf. 94 (2016) 138–144.
[12] A. Sellitto, V.A. Cimmelli, D. Jou, Influence of electron and phonon temperature on the efficiency of thermoelectric conversion, Int. J. Heat Mass Transf. 80 (2015) 344–352.
[13] T. Xue, X. Zhang, K.K. Tamma, On a generalized non-local two-temperature heat transfer DAE modeling/simulation methodology for metal-nonmetal thermal inter-facial problems, Int. J. Heat Mass Transf. 138 (2019) 508–515.
[14] A. Sellitto, I. Carlomagno, M.D. Domenico, Nonlocal and nonlinear effects in hyperbolic heat transfer in a two-temperature model, Zeitschrift für angewandte Mathematik und Physik 72 (1) (2021) 1–15.
[15] A. Bora, W. Dai, J.P. Wilson, J.C. Boyt, Neural network method for solving parabolic two-temperature microscale heat conduction in double-layered thin films exposed to ultrashort-pulsed lasers, Int. J. Heat Mass Transf. 178 (2021) 121616.
[16] S.G. Bezhanov, S.A. Uryupin, Momentum and energy relaxation in femtosecond-scale energy transport in metals, Int. J. Heat Mass Transf. 184 (2022) 122308.
[17] R.E. Gonzalez-Narvaez, M.L. de Haro, F. Vázquez, Internal structure and heat conduction in rigid solids: a two-temperature approach, J. Non-Equilib. Thermodyn. 47 (1) (2022) 13–30.
[18] V.A. Cimmelli, A. Sellitto, D. Jou, Nonlinear evolution and stability of the heat flow in nanosystems: beyond linear phonon hydrodynamics, Phys. Rev. B 82 (18) (2010) 184302.
[19] V.A. Cimmelli, A. Sellitto, D. Jou, Nonlocal effects and second sound in a non-equilibrium steady state, Phys. Rev. B 79 (1) (2009) 014303.
[20] M. Wang, N. Yang, Z.Y. Guo, Non-Fourier heat conductions in nanomaterials, J. Appl. Phys. 110 (6) (2011) 064310.
[21] F.X. Alvarez, D. Jou, Memory and nonlocal effects in heat transport: from diffusive to ballistic regimes, Appl. Phys. Lett. 90 (8) (2007) 083109.
[22] A. Berezovski, M. Berezovski, Influence of microstructure on thermoelastic wave propagation, Acta Mech. 224 (11) (2013) 2623–2633.
[23] S.J. Rogers, Second sound in solids: the effects of collinear and non-collinear three phonon processes, Le Journal de Physique Colloques 33 (4) (1972) 4–111.
[24] T.F. McNelly, Second sound and anharmonic processes in isotopically pure Alkali-Halides, Cornell University, 1974 Ph.D. Thesis.
[25] G. Chen, Ballistic-diffusive heat-conduction equations, Phys. Rev. Lett. 86 (11) (2001) 2297–2300.
[26] I. Müller, T. Ruggeri, Rational Extended Thermodynamics, Springer, 1998.
[27] D.D. Joseph, L. Preziosi, Heat waves, Rev. Mod. Phys. 61 (1) (1989) 41.
[28] M. Szücs, R. Kovács, S. Simić, Open mathematical aspects of continuum thermodynamics: hyperbolicity, boundaries and nonlinearities, Symmetry 12 (2020) 1469.
[29] R. Kovács, Analytic solution of Guyer-Krumhansl equation for laser flash experiments, Int. J. Heat Mass Transf. 127 (2018) 631–636.
[30] R.A. Guyer, J.A. Krumhansl, Solution of the linearized phonon Boltzmann equation, Phys. Rev. 148 (2) (1966) 766–778.
[31] T. Ruggeri, M. Sugiyama, Rational Extended Thermodynamics Beyond the Monatomic Gas, Springer, 2015.
[32] I. Gyarmati, Non-Equilibrium Thermodynamics, Springer, 1970.
[33] P. Ván, Weakly nonlocal irreversible thermodynamics – the Guyer-Krumhansl and the Cahn-Hilliard equations, Phys. Lett. A 290 (1–2) (2001) 88–92.
[34] P. Ván, T. Fülöp, Universality in heat conduction theory – weakly nonlocal thermodynamics, Annalen der Physik 524 (8) (2012) 470–478.
[35] W. Dreyer, H. Struchtrup, Heat pulse experiments revisited, Continuum Mech. Thermodyn. 5 (1993) 3–50.
[36] V. Józsa, R. Kovács, Solving Problems in Thermal Engineering: A Toolbox for Engineers, Springer, 2020.
[37] T. Fülöp, R. Kovács, P. Ván, Thermodynamic hierarchies of evolution equations, Proc. Est. Acad. Sci. 64 (3) (2015) 389–395.
[38] T. Fülöp, R. Kovács, A. Lovas, A. Rieth, T. Fodor, M. Szücs, P. Ván, G. Gróf, Emergence of non-Fourier hierarchies, Entropy 20 (11) (2018) 832. ArXiv: 1808.06858
[39] R. Kovács, P. Rogolino, Numerical treatment of nonlinear Fourier and Maxwell–Cattaneo-Vernotte heat transport equations, Int. J. Heat Mass Transf. 150 (2020) 119281.
[40] J. Ignaczak, M. Ostoja-Starzewski, Thermoelasticity with Finite Wave Speeds, OUP Oxford, 2009.
[41] D.Y. Tzou, Macro- to Micro-scale Heat Transfer: The Lagging Behavior, CRC Press, 1996.

[42] Y. Zhang, Generalized dual-phase lag bioheat equations based on nonequilibrium heat transfer in living biological tissues, Int. J. Heat Mass Transf. 52 (21) (2009) 4829–4834.
[43] J. Zhou, J.K. Chen, Y. Zhang, Dual-phase lag effects on thermal damage to biological tissues caused by laser irradiation, Comput. Biol. Med. 39 (3) (2009) 286–293.
[44] N. Afrin, J. Zhou, Y. Zhang, D.Y. Tzou, J.K. Chen, Numerical simulation of thermal damage to living biological tissues induced by laser irradiation based on a generalized dual phase lag model, Numer. Heat Transf. Part A 61 (7) (2012) 483–501.
[45] M. Fabrizio, F. Franchi, Delayed thermal models: stability and thermodynamics, J. Therm. Stresses 37 (2) (2014) 160–173.
[46] M. Fabrizio, B. Lazzari, Stability and second law of thermodynamics in dual-phase-lag heat conduction, Int. J. Heat Mass Transf. 74 (2014) 484–489.
[47] R. Kovács, P. Ván, Thermodynamical consistency of the dual phase lag heat conduction equation, Continuum Mech. Thermodyn. (2017) 1–8.
[48] R. Quintanilla, R. Racke, Qualitative aspects in dual-phase-lag heat conduction, Proc. R. Soc. London A 463 (2079) (2007) 659–674.
[49] M. Dreher, R. Quintanilla, R. Racke, Ill-posed problems in thermomechanics, Appl. Math. Lett. 22 (9) (2009) 1374–1379.
[50] S.A. Rukolaine, Unphysical effects of the dual-phase-lag model of heat conduction: higher-order approximations, Int. J. Therm. Sci. 113 (2017) 83–88.
[51] C. Cattaneo, Sur une forme de lequation de la chaleur eliminant le paradoxe dune propagation instantanee, C. R. Hebd. Seances Acad. Sci. 247 (4) (1958) 431–433.
[52] P. Vernotte, Les paradoxes de la théorie continue de léquation de la chaleur, C. R. Hebd. Seances Acad. Sci. 246 (22) (1958) 3154–3155.
[53] R. Kovács, Heat conduction beyond Fourier's law: theoretical predictions and experimental validation, Budapest University of Technology and Economics (BME), 2017 PhD thesis.
[54] P.M. Mariano, Mechanics of material mutations, Adv. Appl. Mech 47 (1) (2014) 91.
[55] G. Capriz, K. Wilmanski, P.M. Mariano, Exact and approximate Maxwell-Cattaneo-type descriptions of heat conduction: a comparative analysis, Int. J. Heat Mass Transf. 175 (2021) 121362.
[56] A. Rieth, R. Kovács, T. Fülöp, Implicit numerical schemes for generalized heat conduction equations, Int. J. Heat Mass Transf. 126 (2018) 1177–1182.
[57] W.J. Parker, R.J. Jenkins, C.P. Butler, G.L. Abbott, Flash method of determining thermal diffusivity, heat capacity, and thermal conductivity, J. Appl. Phys. 32 (9) (1961) 1679–1684.